



1 The importance of non-stationary multiannual periodicities in the NAO index for forecasting  
2 water resource extremes

3 William Rust <sup>a</sup>; John P Bloomfield <sup>b</sup>; Mark Cuthbert <sup>cd</sup>; Ron Corstanje <sup>e</sup>; Ian Holman <sup>a</sup>

4 <sup>a</sup> Cranfield Water Science Institute (CWSI), Cranfield University, Bedford MK43 0AL

5 <sup>b</sup> British Geological Survey, Wallingford, OX10 8BB

6 <sup>c</sup> School of Earth and Environmental Sciences, Cardiff University, Park Place, Cardiff, CF10  
7 3AT

8 <sup>d</sup> School of Civil and Environmental Engineering, The University of New South Wales,  
9 Sydney, Australia

10 <sup>e</sup> Centre for Environment and Agricultural Informatics, Cranfield University, Bedford MK43  
11 0AL

12

13 Correspondence to Ian Holman (i.holman@cranfield.ac.uk)

14 **Abstract**

15 Drought forecasting and early warning systems for water resource extremes are increasingly  
16 important tools in water resource management, particularly in Europe where increased  
17 population density and climate change are expected to place greater pressures on water  
18 supply. In this context, the North Atlantic Oscillation (NAO) is often used to indicate future  
19 water resource behaviours (including droughts) over Europe, given its dominant control on  
20 winter rainfall totals in the North Atlantic region. Recent hydroclimate research has focused  
21 on the role of multiannual periodicities in the NAO in driving low frequency behaviours in  
22 some water resources, suggesting that notable improvements to lead-times in forecasting  
23 may be possible by incorporating these multiannual relationships. However, the importance  
24 of multiannual NAO periodicities for driving water resource behaviour, and the feasibility of  
25 this relationship for indicating future droughts, has yet to be assessed in the context of  
26 known non-stationarities that are internal to the NAO and its influence on European  
27 meteorological processes. Here we quantify the time-frequency relationship between the  
28 NAO and a large dataset of water resources records to identify key non-stationarities that  
29 have dominated multiannual behaviour of water resource extremes over recent decades.  
30 The most dominant of these is a 7.5-year periodicity in water resource extremes since  
31 approximately 1970 but which has been diminishing since 2005. Furthermore, we show that



32 the non-stationary relationship between the NAO and European rainfall is clearly expressed  
33 at multiannual periodicities in the water resource records assessed. These multiannual  
34 behaviours are found to have modulated historical water resource anomalies to an extent  
35 that is comparable to the projected effects of a worst-case climate change scenario.  
36 Furthermore, there is limited systematic understanding in existing atmospheric research for  
37 non-stationaries in these periodic behaviours which poses considerable implications to  
38 existing water resource forecasting and projection systems, as well as the use of these  
39 periodic behaviours as an indicator of future water resource drought.

40

## 41 **1. Introduction**

42 Oscillatory ocean-atmosphere systems (such as El Nino Southern Oscillation (ENSO), North  
43 Atlantic Oscillation (NAO) and Pacific Decadal Oscillation (PDO)) are known to modulate  
44 hydrometeorological processes over a large domain, often driving multiannual periodicities in  
45 hydrological records (Kuss and Gurdak, 2014; Labat, 2010; Trigo et al., 2002). As such,  
46 indices of these systems can be useful when explaining decadal-scale variations in water  
47 resource behaviour in Europe (Svensson et al, 2015; Kingston et al, 2006), North America  
48 (Coleman and Budikova, 2013) and Asia (Gao et al, 2021). In the North Atlantic region, the  
49 NAO represents the principal mode of atmospheric variability and is a leading control on  
50 European winter rainfall totals (Hurrell, 1995; Hurrell and Deser, 2010). As such, many  
51 studies have found strong and significant relationships between the winter NAO Index  
52 (NAOI) and hydrological variables across Europe (Wrzesinski and Paluszkiwicz, 2011;  
53 Brady et al, 2019; Burt and Howden, 2013), leading to the development of seasonal and  
54 long-lead forecasting systems of hydrological behaviour (Svensson et al, 2015, Bonaccorso  
55 et al, 2015).

56 A growing number of studies have identified stronger relationships between the NAOI and  
57 certain water resource variables at multiannual periodicities (Holman et al, 2011; Neves et



58 al, 2019; Uvo et al, 2021), than at an annual scale. This is particularly apparent where longer  
59 hydrological response times predominate (Rust et al 2021a). For instance, Neves et al  
60 (2019) identified significant relationships between the NAOI and groundwater level in  
61 Portuguese aquifers and at approximately 6- and 10-year periodicities, with associations to  
62 episodes of recorded groundwater drought. Furthermore, Liesch and Wunsch (2019) found  
63 significant coherence between NAOI and groundwater level at approximately 6- to 16-year  
64 periodicities across the UK, Germany, Netherlands and Denmark. Rust et al (2019; 2021a)  
65 identified a similar significant 6- to 9-year cycle across a large dataset of groundwater level  
66 (59 boreholes) and streamflow (705 gauges) in the UK, which was associated with the  
67 principal periodicity of the NAO (of a similar length (Hurrell et al., 2003; Zhang et al., 2011)).  
68 In the instance of groundwater level, this periodicity was found to represent a notable portion  
69 of overall behaviour (40% the standard deviation), and minima in the cycle were shown to  
70 align with recorded instances of wide-spread groundwater drought (Rust et al, 2019). Given  
71 their association with recorded droughts across Europe, these studies highlight the potential  
72 benefit of an *a priori* knowledge of multiannual NAO periodicities in water resources for  
73 improving preparedness for water resource extremes in Europe. Here we use extremes to  
74 describe water resource deficit (i.e., drought) and periods of anomalously high water  
75 resource stores. This is distinct from hydrological extremes, which infers the drought – flood  
76 continuum.

77 However, the value of a multiannual relationship between the NAO and European water  
78 resources has yet to be assessed in the context of reported non-stationarities in  
79 hydroclimate systems. For instance, the NAO is an intrinsic mode of atmospheric variability  
80 (Deser et al, 2017), but can also be influenced by multiple other teleconnection systems  
81 such as the Madden-Julien Oscillation, Quasi-Biennial Oscillation (Feng et al 2021) or El-  
82 Nino Southern Oscillation (Zhang et al, 2019). As such it is currently unclear whether  
83 periodicities in the NAOI are emergent behaviours or the result of external forcing. This has  
84 been compounded by a relatively weak signal-to-noise ratio for NAO periodicities, making



85 confident multiannual signal detection difficult (O'Reilly et al, 2018; Hurrell et al, 1997). While  
86 stronger NAO-like multiannual periodicities have been detected in water resource variables,  
87 due to the high-band filtering function of hydrological processes (van Loon, 2013), the  
88 degree to which these behaviours are sufficiently stable to enable development of predictive  
89 utilities is currently unclear. Furthermore, existing research has shown that the sign of the  
90 relationship between NAOI and European rainfall is non-stationary at decadal timescales  
91 (Rust et al, 2021b); Vicente-Serrano and López-Moreno (2008)). This is expected to add a  
92 degree of uncertainty to the detection of lead times between multiannual periodic  
93 components in the NAO and water resource response, which is necessary in the  
94 development of early warning systems for water resource extremes. While some studies  
95 have ascribed lags to this multiannual relationship for European water resources (Neves et  
96 al, 2019; Holman et al, 2011), the extent to which this non-stationarity is present at  
97 multiannual periodicities has yet to be assessed.

98 Finally, a critical application of early warning systems for water resource extremes is in the  
99 design of drought management regimes for existing and projected climate change (Sutanto  
100 et al, 2020). While some studies have quantified the degree of modulation that multiannual  
101 ocean-atmosphere systems can have on water resources (Kuss and Gurdak, 2014; Neves et  
102 al., 2019; Velasco et al., 2015), few have compared these to the expected modulations from  
103 projected climate change scenarios. As such the benefit of incorporating multiannual NAO  
104 periodicities into early warning systems for improving preparedness for water resource  
105 extremes in climate change scenarios has not been assessed.

106 The aim of this paper is to assess the utility of multiannual relationships between the NAO  
107 and water resources for improving preparedness for future water resource extremes. This  
108 aim will be met by addressing the following research objectives:

- 109 1. Quantify significant covariances between multiannual periodicities in the NAOI and  
110 water resource extremes, and assess the extent to which these periodicities are  
111 stable over time



- 112        2. Assess multiannual periodicity phase differences between the NAOI and water  
113            resources over time, to understand the extent to which annual-scale non-  
114            stationarities between the NAO and European rainfall are expressed at multiannual  
115            scales
- 116        3. Quantify the modulations of water resource variables caused by key multiannual  
117            periodicities in the NAO, during the dry season, and compare this with projected  
118            modulations of water resources due to climate change.

119    These objectives will be implemented on UK water resource records, given the considerable  
120    coverage of recorded water resource data in time and across the space (Marsh and  
121    Hannaford, 2008); however, the methodologies developed can be applied to any regions.

122

## 123    **2. Data**

### 124    2.1.    Water resource data

125    The National Groundwater Level Archive (NGLA) and National River Flow Archive (NRFA)  
126    provide high-resolution spatiotemporal coverage of groundwater level records and  
127    streamflow across the UK.

#### 128    2.1.1.    Groundwater data

129    Monthly NGLA groundwater level data from 136 boreholes covering all of the major UK  
130    aquifers, with record lengths of more than 20 years and data gaps no longer than 24 months,  
131    have been used (Figure 1). While some meta-analysis was conducted on monthly data, the  
132    primary analysis was undertaken on seasonally averaged data, meaning a data gap of no  
133    more than two points. They cover a range of unconfined and confined consolidated aquifer  
134    types and have been categorised into generalised aquifer groups of Chalk (78 sites),  
135    Limestone (12 sites), Oolite (12 sites), Sandstone (34) and variably cemented mixed clays  
136    and sands (Lower Greensand Group, Allen et al., 1997) (3 sites). Given the spatially  
137    heterogenous response of the Chalk aquifer to droughts (Marchant and Bloomfield, 2018),



138 Chalk sites have been subdivided into four groups based on aquifer region: Lincolnshire basin  
139 (8 sites), East Anglian basin (17 sites), Thames and Chiltern basin (29 sites) and Southern  
140 basin (21 sites) (Allen et al., 1997; Marchant and Bloomfield, 2018).

141 Broad aquifer groups can be described as follows: Chalk, a limestone aquifer comprising of a  
142 dual porosity system with localized areas where it exhibits confined characteristics;  
143 characterised by fast-responding fracture porosity (Bloomfield, 1996); Oolite characterised by  
144 a highly fractured lithology with low intergranular permeability; Sandstone, comprised of sands  
145 silts and muds with principle inter-granular flow but fracture flow where fractures persist; and  
146 Lower Greensand, characterised by intergranular flow with lateral fracture flow depending on  
147 depth and formation (Allen et al, 1997).

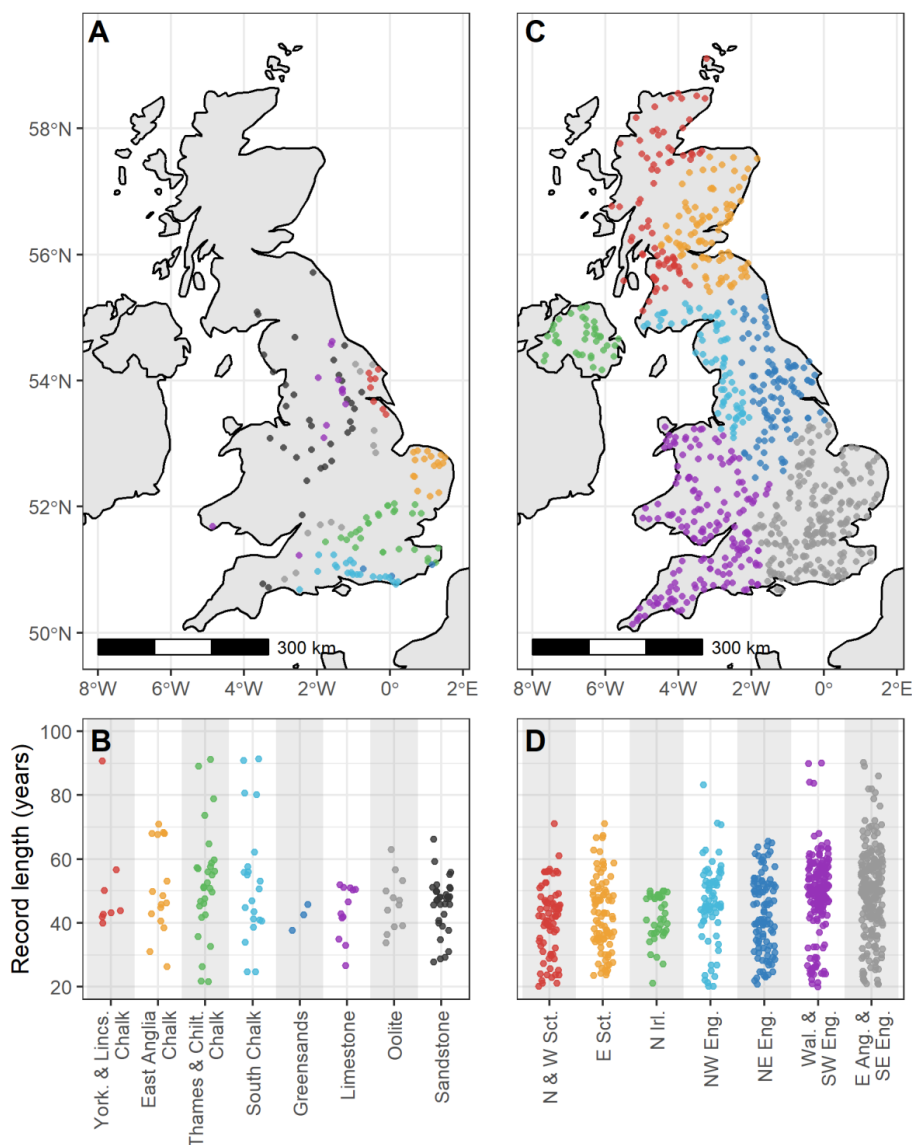
#### 148 2.1.2. Streamflow data

149 Monthly streamflow data from the UK National River Flow Archive (NRFA; Dixon et al., 2013:  
150 <http://nrfa.ceh.ac.uk/>) has been used. Gauging stations with more than 20 years of continuous  
151 streamflow data and no data gaps greater than 24 months were initially selected. Sites serving  
152 the largest catchment were selected where there are multiple sites within a single river  
153 catchment. This produced a final list of 767 streamflow gauging stations for use. To  
154 understand broad spatial relationships across the streamflow dataset, records have been  
155 divided into groups based on the NRFA river drainage basin (RDB). These are grouped by  
156 seven generalised regions of the UK; North and West Scotland (75 records), East Scotland  
157 (89 records), Northern Ireland (38 records), North-west England (70 records), North-east  
158 England (102 records), Wales & South-west England (170 records), East Anglia & South-east  
159 England (223 records). Streamflow with minimal influence from human factors is often used  
160 in hydroclimate studies to avoid confounding mechanisms, however no such large-scale  
161 dataset exists for the UK. Furthermore, over the period of analysis and the broad scale of this  
162 assessment, inconsistencies in the way water resource management practices are  
163 implemented is expected to result in noise to the observations rather than some systematic  
164 signal or bias that would affect the results of this paper.



165 2.2. North Atlantic Oscillation data

166 Monthly North Atlantic Oscillation Index (NAOI) data calculated by the National Centre for  
167 Atmospheric Research (NCAR) using the principal component (PC) method for the period  
168 1989 – 2021 has been used. The PC NAOI is a time series of the leading empirical orthogonal  
169 functions (EOFS) of sea level pressure grids across the north Atlantic region (20°-80°N, 90°W-  
170 40°E).



171

172 Figure 1 – Spatial and temporal distributions of water resource records; a) location of  
 173 groundwater boreholes coloured by associated aquifer group, b) jitter plot of groundwater  
 174 record lengths within each aquifer group, c) location of streamflow gauges coloured by  
 175 associated regional group, d) jitter plot of streamflow record lengths within each regional group

176

177





178 **3. Methods**

179 **3.1. Data Pre-processing**

180 In this study we use the continuous and cross-wavelet transform to understand behaviours  
181 and relationships across different periodicities within the different water resource variable time  
182 series.

183 For all datasets, gaps less than two years were infilled to a monthly time step using a cubic  
184 spline to produce a complete time series for the wavelet transform. For time series with gaps  
185 greater than two years, the shortest time period before or after the data gap was removed.  
186 The records were not trimmed to obtain a common period of data coverage. Instead, all data  
187 was trimmed to start at a minimum of 1930. This was to allow the analysis of the fewer records  
188 that cover a longer time period while still capturing a time periods with adequate record  
189 coverage. All of the time series were standardised by dividing by their standard deviation and  
190 subtracting their mean.

191 **3.2. Quantifying wide-spread water resource extremes**

192 In order to meet objective 1, we produced a time series which describes the behaviour of  
193 wide-spread water resource extremes across each resource variable (i.e., groundwater or  
194 streamflow). In this study we have assessed water resource extremes using a drought  
195 threshold methodology proposed in Peters (2003). While other measures of drought are  
196 available (e.g., Standardised Precipitation Index (SPI) and Standardised Groundwater Index  
197 (SGI)) (Bloomfield and Marchant, 2013), a threshold approach has been adopted as its can  
198 be easily applied to both streamflow and groundwater variables.

199 To calculate a drought series from monthly groundwater level and streamflow series, we first  
200 used the threshold methodology given by equation 4.3 in Peters (2003):

201



$$\int_0^M (x_t(c) - x(t))_+ dt = c \int_0^M (\bar{x} - x(t))_+ dt \quad (\text{Eq. 5})$$

202 Where:

$$203 \quad x_+ = \begin{cases} x & \text{if } x \geq 0 \\ 0 & \text{if } x < 0 \end{cases}$$

204 and  $M$  is the full length of the data series. Here we use a threshold level of  $c = 0.3$  for  
205 groundwater level and  $c = 0.01$  for streamflow. Peters et al (2003) found that a value of 0.3  
206 for groundwater level was comparable to other commonly used thresholds. A value of 0.01  
207 for streamflow was chosen as it produced a similar distribution of drought events as the  
208 groundwater drought series. The chosen value of  $c$  for either variable is not expected to  
209 affect the outcomes of the study as the focus is on the frequency structure of water resource  
210 extremes, rather than magnitude.

211 For each measurement site, the monthly time series of drought status (whether in drought  
212 according to the threshold criteria or not) was converted into a yearly series describing  
213 whether that site experienced a drought in the calendar year. Then, for each year, the  
214 number of sites that experienced drought were summed and divided by the number of sites  
215 with coverage of that year. This produced a time series of the proportion of sites  
216 experiencing drought each year, for groundwater level and streamflow variables. This is  
217 referred to as the drought coverage time series.

### 218 **3.3. Frequency Transformations**

#### 219 **3.3.1. Continuous Wavelet Transform (CWT)**

220 The Continuous Wavelet Transform (CWT) was performed on the drought coverage time  
221 series for groundwater and streamflow to understand the frequency behaviour of wide-  
222 spread water resource extremes over time. The CWT is often used in geoscience to  
223 understand non-stationarities of a variable over time and frequency space (Sang, 2013).



224 The cross-wavelet transform,  $W$ , consists of the convolution of the data sequence ( $x_t$ ) with  
225 scaled and shifted versions of a mother wavelet (daughter wavelets):

$$W(\tau, s) = \sum_t x_t \frac{1}{\sqrt{s}} \psi * \left( \frac{t - \tau}{s} \right) \quad (\text{Eq. 1})$$

226 where the asterisk represents the complex conjugate,  $\tau$  is the localized time index,  $s$  is the  
227 daughter wavelet scale and  $dt$  is increment of time shifting of the daughter wavelet. The  
228 choice of the set of scales  $s$  determines the wavelet coverage of the series in its frequency  
229 domain. The Morlet wavelet was favoured over other candidates due to its good definition in  
230 the frequency domain and its similarity with the signal pattern of the environmental time  
231 series used (Tremblay et al. 2011; Holman et al. 2011).

232 The modulus of the transform can be interpreted as the continuous wavelet power (CWP):

$$P(\tau, s) = |W(\tau, s)| \quad (\text{Eq. 2})$$

233 We use the package “WaveletComp” produced by Rosch & Schmidbauer (2018) for all  
234 wavelet transformations in this paper.

### 235 **3.3.2. Cross-Wavelet Transform (XWT)**

236 The bivariate XWT was applied between the NAOI and each of the water resources records  
237 (groundwater level (GWL) and streamflow (SF)). This produces a cross-wavelet power which  
238 is analogous to the covariance between the two variables over a time and frequency  
239 spectrum. This has been selected over the cross-wavelet coherence (analogous to  
240 correlation) as this metric requires a high degree of spectral smoothing, making the resultant  
241 coherence spectra sensitive to the choice of smoothing approach (Rosch & Schmidbauer  
242 (2018)) Here we use the covariance spectrum to compare against the drought series  
243 frequency spectrum to understand where strong coherences are reflective of dominant  
244 behaviours in water resource extremes.



245 In order to calculate cross-wavelet power (XWP) for the bivariate case, it is first necessary to  
246 calculate the continuous wavelet transform (CWT) for each of the variables separately. The  
247 XWT between variables  $x$  and  $y$  is given by:

$$W.xy(\tau, s) = \frac{1}{s} \cdot W.x(\tau, s) \cdot W.y^*(\tau, s) \quad (\text{Eq. 3})$$

248 The modulus of the transform can be interpreted as the cross-wavelet power (XWP):

$$P.xy(\tau, s) = |W.xy(\tau, s)| \quad (\text{Eq. 4})$$

249

### 250 3.3.3. Wavelet Significance

251 Lag-1 autocorrelations (AR1) in environmental datasets can produce emergent low frequency  
252 behaviours, making the detection of externally-forced behaviours more difficult (Allen and  
253 Smith, 1996; Meinke et al., 2005; Velasco et al., 2015). In this study, a significance test was  
254 undertaken to test the red-noise null hypothesis that wavelet powers calculated are the result  
255 of the recorded variables' AR1 properties. This was based on 1000 synthetic Monte Carlo  
256 series with the original AR1 values. In this paper we test significance to the 95% CI.

257 The significance spectra for the XWT for each variable pair (e.g., GWL and NAOI) form the  
258 primary results for the XWT method in this paper, since the cross-wavelet power is heavily  
259 dependent on the individual series and its frequency composition. The overall relationship  
260 between the NAOI and water resources as a whole are investigated by showing the proportion  
261 of sites over time and frequency that exhibit a significant relationship with the NAOI (95% CI).  
262 This average significance spectrum is produced by summing the significance matrices across  
263 each resource (groundwater level or streamflow) and dividing by the number of records used  
264 in year each.

265

### 266 3.3.4. Phase Difference



267 In the bivariate case, the instantaneous phase difference for the XWP spectrum (between  
268 wavelets pairs from the CWT spectrum for each variable) can also be calculated as:

$$\text{Angle}(\tau, s) = \text{Arg}(W_{xy}(\tau, s)) \quad (\text{Eq. 5})$$

269

270 This is the difference of the individual phases from both variables at an instantaneous time  
271 and frequency (period), converted to an angle between  $-\pi$ , and  $\pi$ . Values close to 0 indicate  
272 the two series move in-phase, with absolute values close to  $\pi$  indicating an out-of-phase  
273 relationship. Values between 0 and  $\pi$  indicate degrees of phase difference or phase shift.  
274 Phase differences between 0 and  $\pi$  can indicate the degree to which variable x is leading  
275 variable y, however a phase difference between 0 and  $-\pi$  can either indicate that variable y is  
276 leading variable x, or that variable x is leading by more than half the phase rotation (period  
277 length). The degree to which a certain variable is leading is analogous to a lag between the  
278 two variables.

279

### 280 3.4. Modulation measurement

281 In order to understand the degree of modulation that the NAO teleconnection has on water  
282 resources, an absolute and relative modulation value has been calculated for each series.  
283 Here, we use modulation to describe the degree to which the NAO (or other process) has  
284 increased or decreased a water resource measure from its mean. This has been derived by  
285 reconstructing a specific principal periodicity range from the cross-wavelet powers using the  
286 following equation:

$$(x_t) = \frac{dj \cdot dt^{1/2}}{0.776 \cdot \psi(0)} \sum_s \frac{\text{Re}(W(., s))}{s^{1/2}} \quad (\text{Eq. 6})$$

287 Where dj is the frequency step and dt is the time step.



288 This produces a periodic reconstruction of a component of the original dataset that conforms  
289 to the set of periodicities (scale steps) selected. The mean and maximum amplitude of this  
290 periodic reconstruction was calculated from the absolute values of minima and maxima.  
291 Since the data were standardised by dividing by the standard deviation prior to the wavelet  
292 transform, this calculated mean and maximum amplitude are also relative to the sd of the  
293 original data. Multiplying the calculated amplitude by the original sd converts this back into a  
294 real-valued measurement. This was only done for groundwater, since streamflow is highly  
295 dependent on catchment size. In the case of streamflow, amplitudes are reported as relative  
296 to the standard deviation of the streamflow record. All calculated modulations were produced  
297 using reconstructed wavelets from after 1970 where the majority of records are present in  
298 both groundwater and streamflow variables. This was done to mitigate the effect of differing  
299 record lengths.

300

## 301 **4. Results**

### 302 **4.1. Multiannual water resource extremes covariance with NAOI**

303 Figure 2 shows the NAOI covariance significance spectrum (fig 2a and 2b) and drought  
304 frequency spectrum (fig 2c and 2d) for the groundwater level records. These have been  
305 plotted together to allow for easier interpretation and comparison of the results. Black lines in  
306 the spectral plots show the 95% CI. The calculated drought series (fig 2e) and record  
307 coverage (fig 2f) have also been plotted alongside for comparison.

308 Figure 2a shows the results from the XWT significance testing between the NAOI and the  
309 136 groundwater level records. Results are displayed as contours showing the percentages  
310 of sites that exhibited a significant (0.05  $\alpha$ ) XWP within the time-frequency spectrum. There  
311 are five localised regions within the NAOI x GWL XWP spectrum that denote a wide-spread  
312 significance between the GWL records and the NAOI. The greatest significance contours of  
313 these regions (referred to here as focal points (FPs)) are labelled on figure 2a as: FP 1: 1934



314 at the 4.2 years periodicity (80% of records); FP 2: 1974 at the 8.5 years periodicity (40% of  
315 records); FP 3: 1995 at 5.4 years (80% of records); FP 4: 2005 at 7 years (90% of records)  
316 and; FP 5: 2012 at 2.9 years (60% of records).

317 These focal points are grouped into three larger regions within the 10% contour; between  
318 1933 – 1940 spanning the 3- to 5-year periodicity; 1964 – 2020 spanning the 4- to 12-year  
319 periodicity and; 2007 – 2017 spanning the 2- to 4-year periodicity. There is a single peak in  
320 the time-averaged percentage plots (figure 2b) at the 7.5-year periodicity (average of 26% of  
321 records)

322 Figure 2c shows the results from the CWT of the groundwater drought series (shown in Fig  
323 2e). There are five regions of significant wavelet power in the groundwater drought  
324 frequency spectrum that are labelled in figure 2c as follows; region 1: 1930 - 1950 in the 4-  
325 to 8-year periodicity range (greatest power at 4.8 years); region 2: 1930 – 1945 in the 10- to  
326 13-year periodicity range (greatest power at 11.7 years); region 3: 1960 – 1965 in the 2.5- to  
327 3.5-year periodicity range (greatest power at 2.8 years); region 4: 1960 – 1990 centred at the  
328 12- to 17-year periodicity range (greatest power at 15.4 years); and region 5: 1980 to 2020  
329 at the 6- to 8-year periodicity range (greatest power at 7 years). There is a sixth significant  
330 region starting in 2019 and covering periods between 2 and 5 years, however this is very  
331 close to the end of the record and may be subject to edge effects. As such this region has  
332 not been taken forward for discussion.

333 There are also two notable non-significant regions of medium strength wavelet power ( $\geq$   
334 0.4); 1930 - 2000 at the 14- to 23-year periodicity range (centred at 16 years), and between  
335 1960 and 1970 at the 8- to 16-year periodicity range (centred at 9 years). There are two  
336 notable peaks in time-averaged wavelet power for the GWL drought series (figure 2d); the  
337 greatest at the 7-year periodicity (average wavelet power of 0.38), and the second at the 14-  
338 year periodicity (average wavelet power of 0.24).



339 Figure 3 shows the same as Figure 2 but for the streamflow (SF) case. There are six  
340 localised regions within the NAOI x SF XWP spectrum that denote a wide-spread  
341 significance between the SF records and the NAOI. FPs of these regions are labelled on  
342 figure 2a; FP 1: 1940 at the 6.7-year periodicity (30% of records); FP 2: 1962 at the 5.2-year  
343 periodicity (50% of records); FP 3: 1975 at the 8.5-year periodicity (40% of records); FP 4:  
344 1994 at the 5.2-year periodicity (80% of records); FP 5: 2007 at the 7-year periodicity (90%  
345 of records) and; FP 6: 2011 to 2015 at the 3.2-year periodicity (60% of records). These  
346 centres are grouped into larger regions within the 10% contour; these are between 1933 –  
347 1947 spanning the 5.5- to 8-year periodicity; 1960 – 1970 spanning the 4- to 8-year  
348 periodicity; 1965 – 1990 spanning the 7- to 11-year periodicity; 1988 – 2000 spanning the 4-  
349 to 5.5-year periodicity; 1995 – 2020 spanning the 4.5- to 11-year periodicity and 2007 –  
350 2017 spanning the 2.5- to 4.5-year periodicity. There is a single peak in the time-averaged  
351 percentage plots (figure 3b) at the 7.5-year periodicity (average of 29% of records)

352 Figure 3c shows the results from the CWT of the streamflow drought series (shown in Fig  
353 3e). There are three regions of significant wavelet power in the groundwater drought  
354 frequency spectrum that are labelled on Figure 3c; region 1: 1930 – 1935 in the 21 year  
355 periodicity (this region appears clipped by the record start date, so the strongest wavelet  
356 power for this region may not be captured); region 2: 1930 - 1937 in the 2.5- to 6.5-year  
357 periodicity range (strongest power at 4.3 years) and; region 3: 1930 – 1960 in the 11- to 15-  
358 year periodicity range (strongest power at 13 years);

359 There are four non-significant regions of medium strength wavelet power ( $\geq 0.4$ ); 1935 –  
360 1945 at the 2- to 3-year periodicity; 1955 – 1965 at the 2- to 4-year periodicity; 1960 – 2015  
361 at the 5.5- to 8-year periodicity; and 2000 – 2005 at the 2- to 5-year periodicity. The time-  
362 averaged wavelet power for the SF drought series (figure 3d) contains multiple peaks  
363 suggesting no dominant periodicity. The greatest peak is at the 7-year periodicity with an  
364 average wavelet power of 0.21.

#### 365 4.2. Cross-wavelet phase difference





366 The cross-wavelet phase difference ( $\phi$ ) between water resource variables and the NAOI at  
367 the 7.5-year periodicity has been displayed in figure 4 for the GWL records and figure 5 for  
368 the streamflow records. The phase difference is a circular measurement where 0 indicates  
369 an in-phase relationship (analogous to zero lag) and  $\pm \pi$  indicates an out-of-phase  
370 relationship between the selected periodicity within the two variables (analogous to half a  
371 periodicity lag (3.75-years)). The purpose of these plots of phase differences are to visualise  
372 and understand the difference in phase between the NAO and water resources. Records  
373 have been split by their aquifer group in Figure 4, and by catchment region in figure 5, to  
374 understand if there are any general differences between regions.

375 The majority of groundwater level records cover the period 1970 to present, meaning  
376 general trends are more clearly presented for this time period. The phase difference of most  
377 GWL records can be defined by a sudden shift at approximately 1990 (figure 4). Values of  $\phi$   
378 generally range from between  $-1/4\pi$  and  $-3/4\pi$  ( $-0.76$  to  $-2.36$  rads; generally anti-phase) for  
379 the period 1975 to 1990 to between  $+1/4\pi$  and  $+3/4\pi$  ( $0.76$  to  $2.36$  rads; generally in-phase)  
380 for the period 1990 to 2019 across all sites. This is with the exception of 17 sites across the  
381 South Chalk and Thames & Chiltern Chalk which have shorter ~anti-phase periods (between  
382 approximately 1985 and 1990). Average  $\phi$  values for the period 1970 – 1990 (1990 – 2020)  
383 for each aquifer region are:  $-1.26$  (1.41) in East Anglian Chalk;  $-2.25$  (1.21) in Lincolnshire  
384 Chalk,  $0.52$  (0.83) in South Chalk,  $-1.37$  (0.83) in Thames & Chiltern Chalk,  $1.51$  (1.21) in  
385 Greensands,  $-0.78$  (0.66) in Limestone,  $-1.36$  (1.09) in Oolite,  $-0.70$  (1.35) in Sandstone. As  
386 such most aquifer regions experience an average reversal of polarity at 1990. Greensand  
387 GWL show no reversal when assessing average  $\phi$  values, however 1 of the 3 sites in this  
388 aquifer group does show this reversal.

389 Similar to the GWL records, most SF records exhibit a shift in phase difference at  
390 approximately 1990, with catchment groups in the north of the UK showing minimal shifts  
391 (i.e., NW Scotland, E Scotland, NI, and NW England) (figure 5). In the southern catchment  
392 groups, values of  $\phi$  generally range from between  $-1/2\pi$  and  $\pm\pi$  (generally anti-phase) for



393 the period 1970-1990 (approximately prior to the shift) to between 0 and  $+3/4\pi$  (generally in-  
394 phase) for the period 1990 to 2020 (approximately after the shift). Furthermore, catchment  
395 groups in the east of the UK (i.e., E Scotland, NE England, East Anglia & SE England)  
396 during the in-phase period (1990-2020) exhibit a notable transition to increased phase  
397 difference (to approximately  $+3/4\pi$ ) between 2000 and 2010 before decreasing to  
398 approximately  $+1/4\pi$  in 2020. Average  $\phi$  values for the period 1970 – 1990 (1990 – 2020)  
399 for each catchment region are: -0.21 (0.14) in North and West Scotland, 0.49 (0.86) in East  
400 Scotland, -0.43 (0.46) in Northern Ireland, -0.44 (0.47) in NW England, 2.32 (1.08) in NE  
401 England, 0.77 (0.64) in Wales and SE England, and 2.53 (0.99) in East Anglia and SE  
402 England.

#### 403 **4.3. Modulation of dry season water resources**

404 Figure 6 shows two boxplots for each aquifer group, representing the distribution of mean (in  
405 blue) and maximum (in red) dry-season GWL deviation as a result of the 7.5-year periodicity  
406 (over the length of each of the record). Median values from each of these mean and  
407 maximum boxplots are described below, and are referred to as med.mean and med.max  
408 respectively.

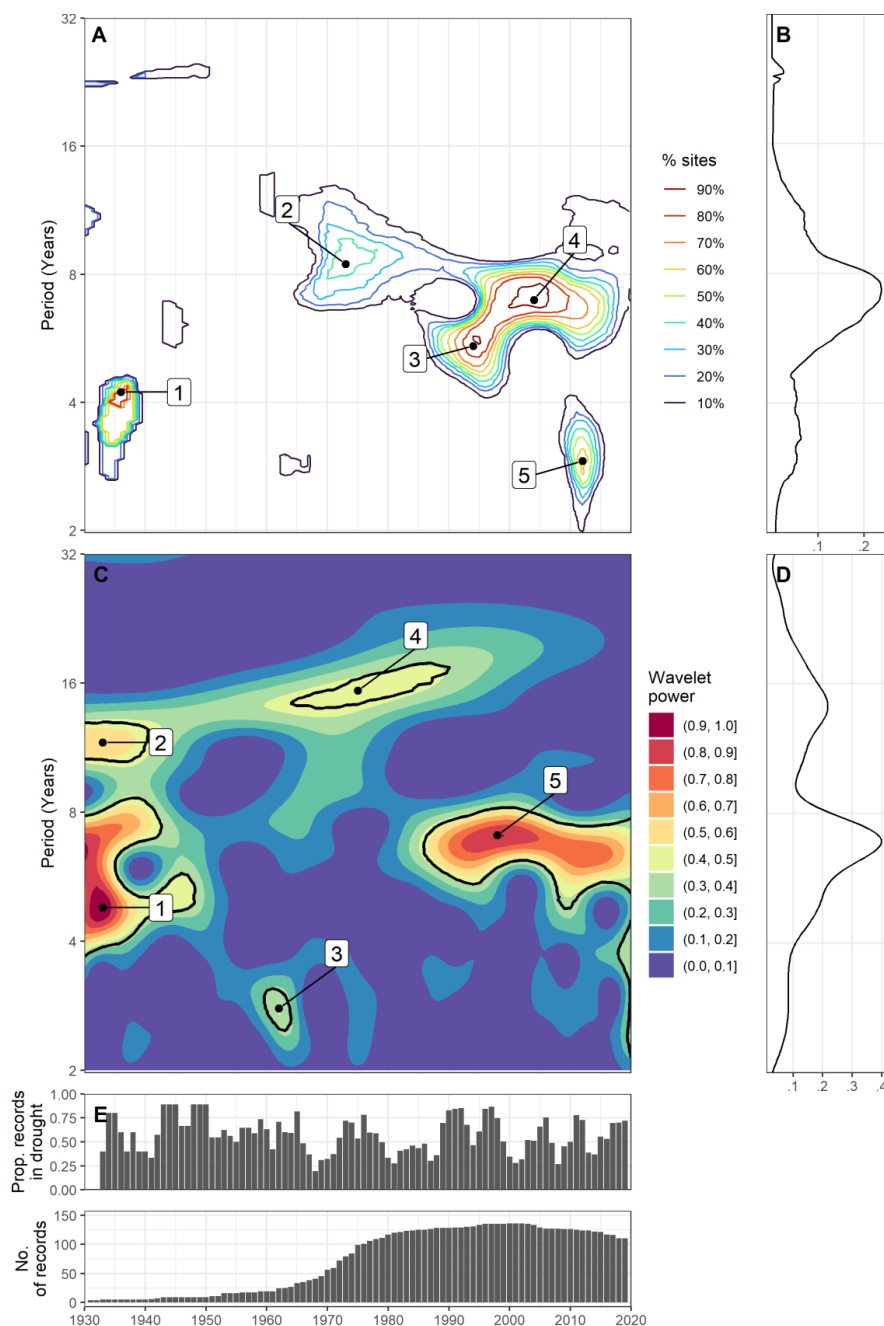
409 The 7.5 year periodicity accounts for the greatest deviation of-dry season GWL in the Chalk  
410 aquifer regions, with the Thames & Chiltern basin GWL showing the greatest modulation of  
411 all groups showing med.mean of 0.94m and a med.max of 1.38m. Two other Chalk groups  
412 showed similarly strong modulations; the South Chalk basin GWL (med.mean: 0.7m,  
413 med.max: 1.07m); and the Lincolnshire Chalk GWL (med.mean: .56m, med.max: 0.77m).  
414 The East Anglia GWL show lowest modulation of the Chalk (med.mean: 0.16m, med.max:  
415 0.34m), similar to GWL in the Limestone (med.mean: 0.35m, med.max: 0.51m) and the  
416 Oolite (med.mean: 0.21m, med.max: 0.33m). Lowest overall modulations are found in the  
417 Sandstone (med.mean: 0.15m, med.max: 0.25m) and Greensands aquifers (med.mean:  
418 0.12m, med.max: 0.17m).



419 Figure 7 shows the same as figure 6 but for the streamflow case. Streamflow modulations  
420 are measured as relative to the standard deviation of each record. Modulation of streamflow  
421 for each catchment group are (in descending order of med.mean); Wales & south-west  
422 England (med.mean: 0.32, med.max: 0.50); East Anglia & south-east England (med.mean:  
423 0.31, med.max: 0.53); Northern Ireland (med.mean: 0.29, med.max: 0.50); West Scotland  
424 (med.mean: 0.27, med.max: 0.46); north-east England (med.mean: 0.27, med.max: 0.47),  
425 north-west England (med.mean: 0.26, med.max: 0.46), east Scotland (med.mean: 0.21,  
426 med.max: 0.39).

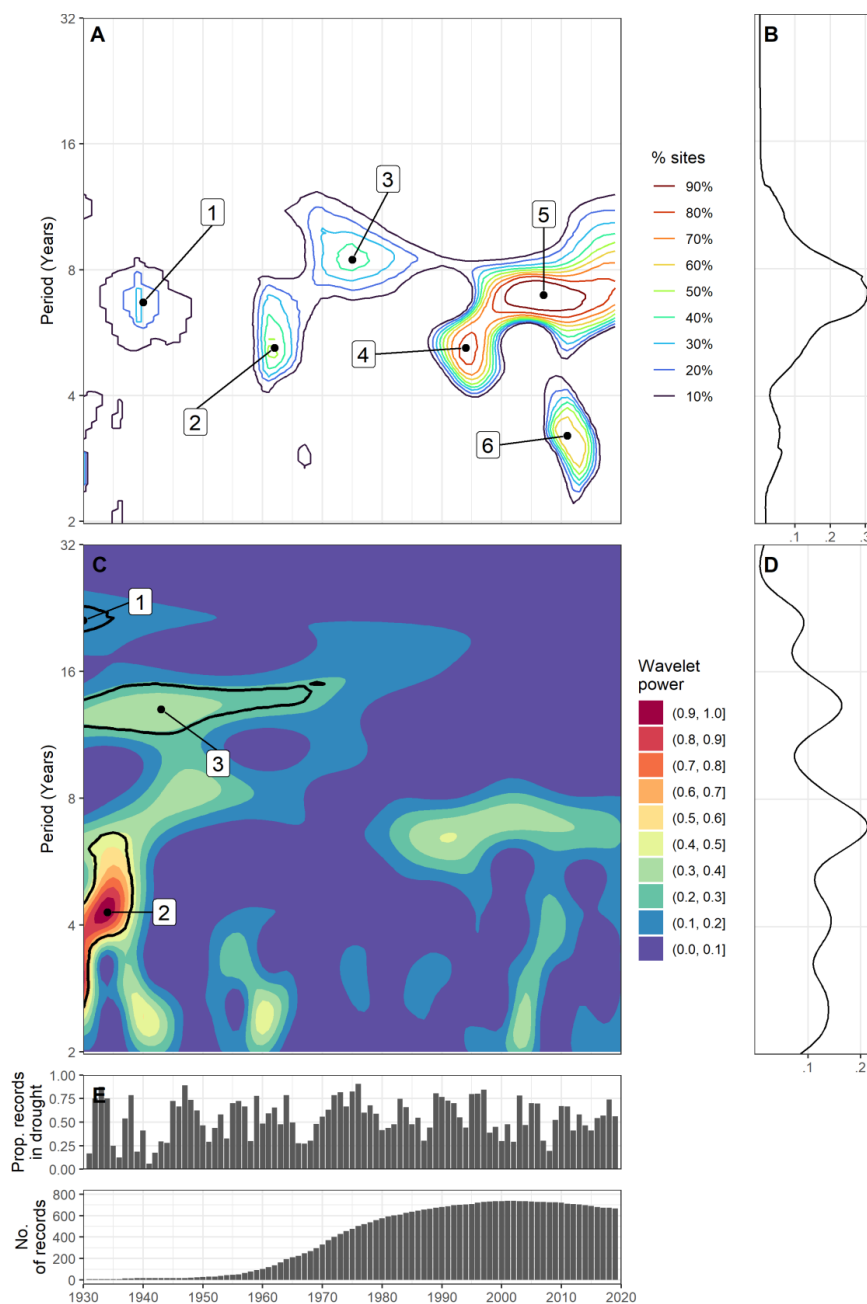
427

428



429

430 Figure 2 – a) Significance (95% CI) contours between GWL and NAOI, b) time-averaged  
 431 proportion of gwl records with a significant XWP with the NAOI (measured as a decimal  
 432 fraction), c) wavelet (spectral) power of GWL drought series, d) time-averaged wavelet  
 433 (spectral) power of GWL drought series, e) GWL drought coverage time series, f) temporal  
 434 coverage of records.



435

436 Figure 3 – a) Significance (95% CI) contours between SF and NAOI, b) time-averaged  
 437 proportion of SF records with a significant XWP with the NAOI (measured as a decimal  
 438 fraction), c) wavelet (spectral) power of SF drought series, d) time-averaged wavelet  
 439 (spectral) power of SF drought series, e) SF drought series showing proportion of records in  
 440 drought each year, f) temporal coverage of records.

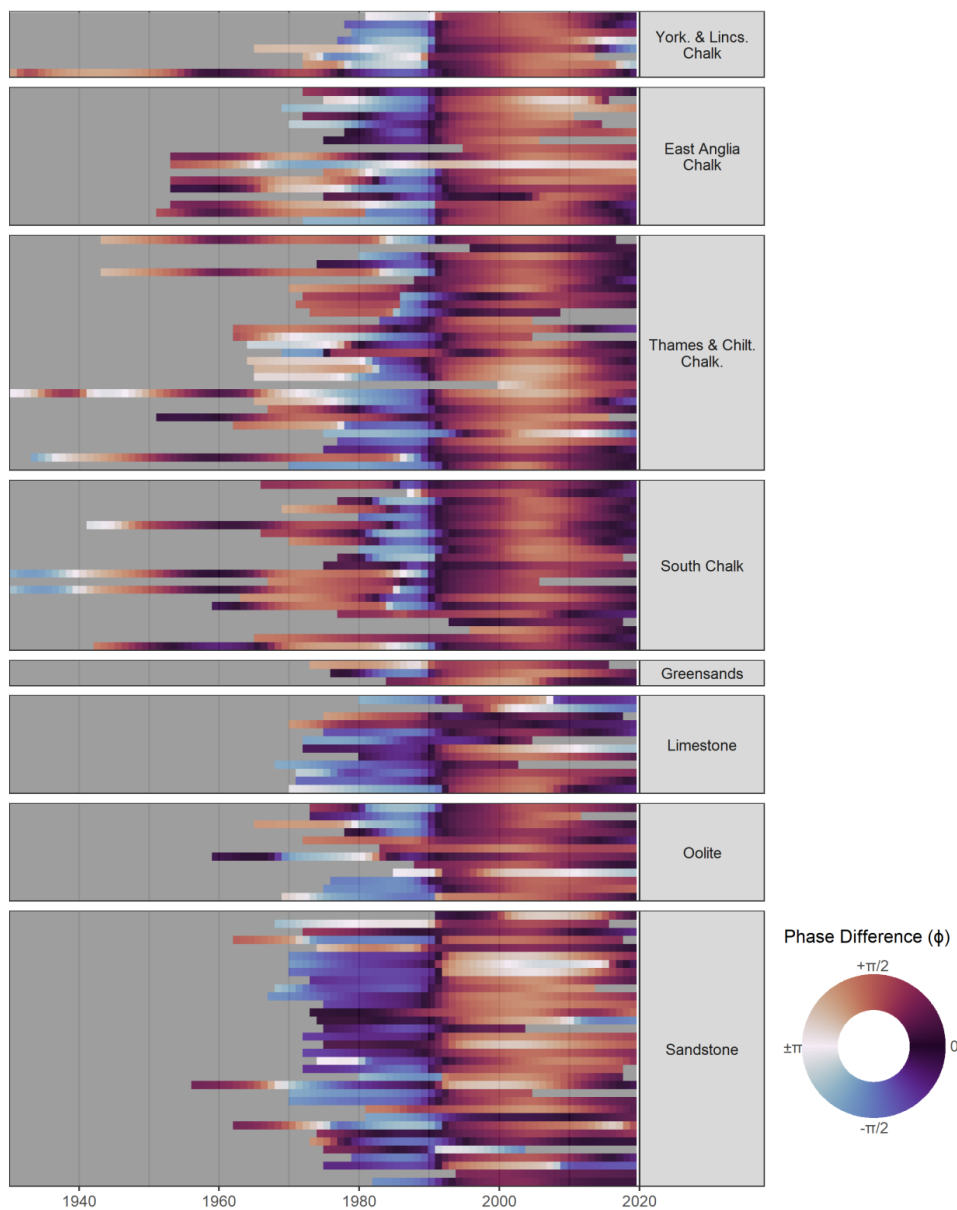
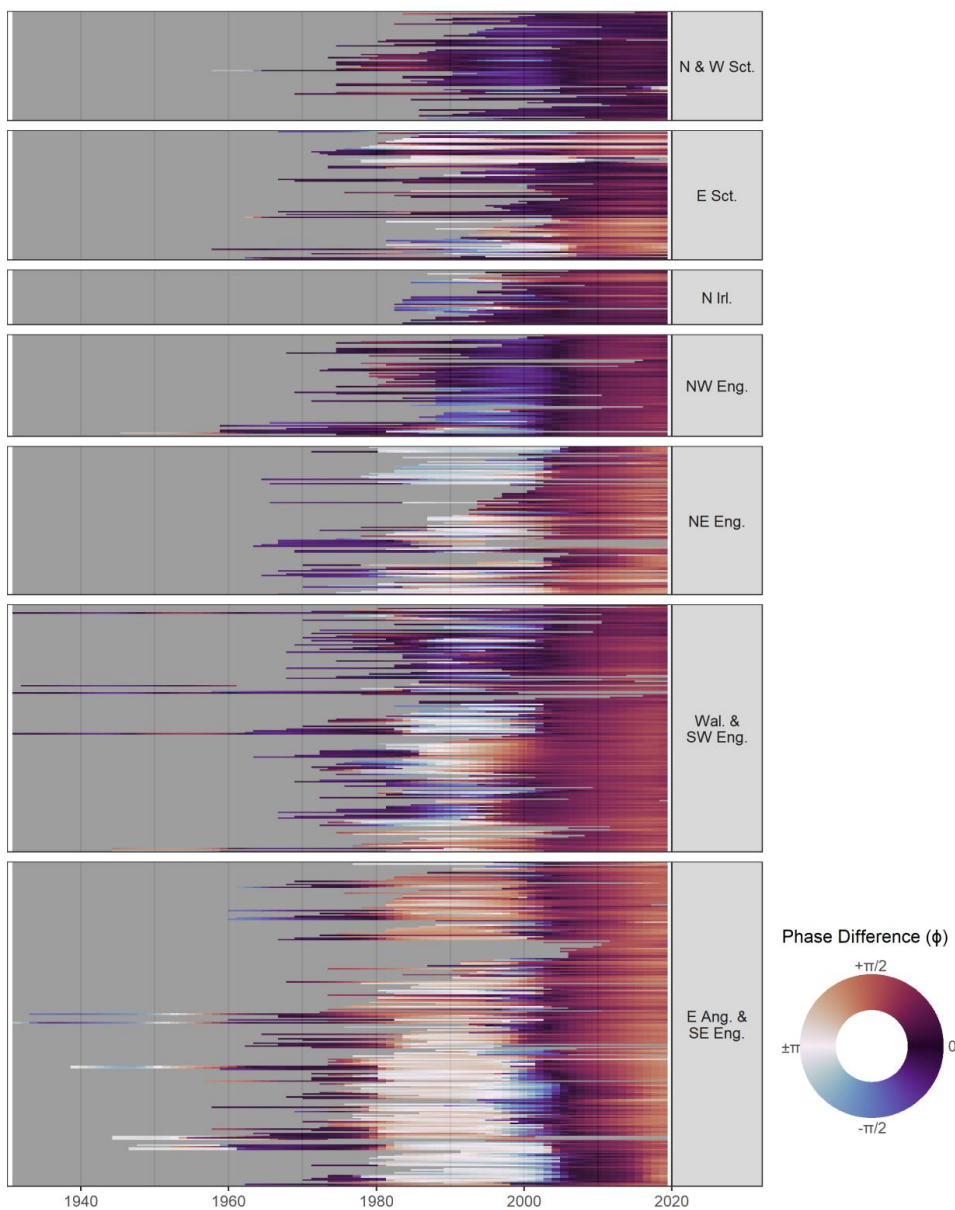


Figure 4 – Phase difference between the NAOI and each GWL record for the GWL record period. Results are grouped by aquifer regions.  $\phi = 0$  is equivalent to an in-phase relationship and  $\phi = \pm\pi$  is equivalent to an antiphase relationship.



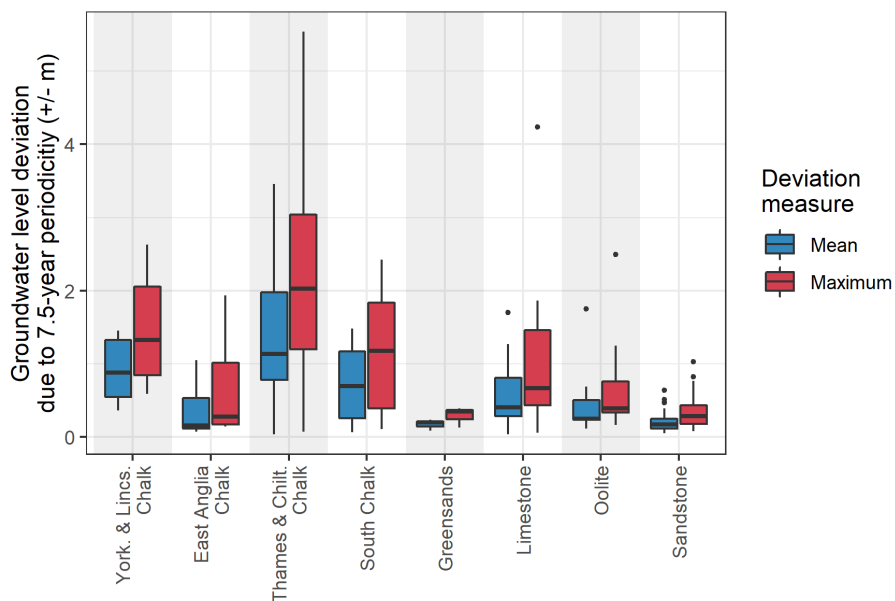
446

447 Figure 5 – Phase difference between the NAOI and each streamflow record for the  
448 streamflow record period. Results are grouped by regions.  $\phi = 0$  is equivalent to an in-phase  
449 relationship and  $\phi = \pm\pi$  is equivalent to an antiphase relationship.

450

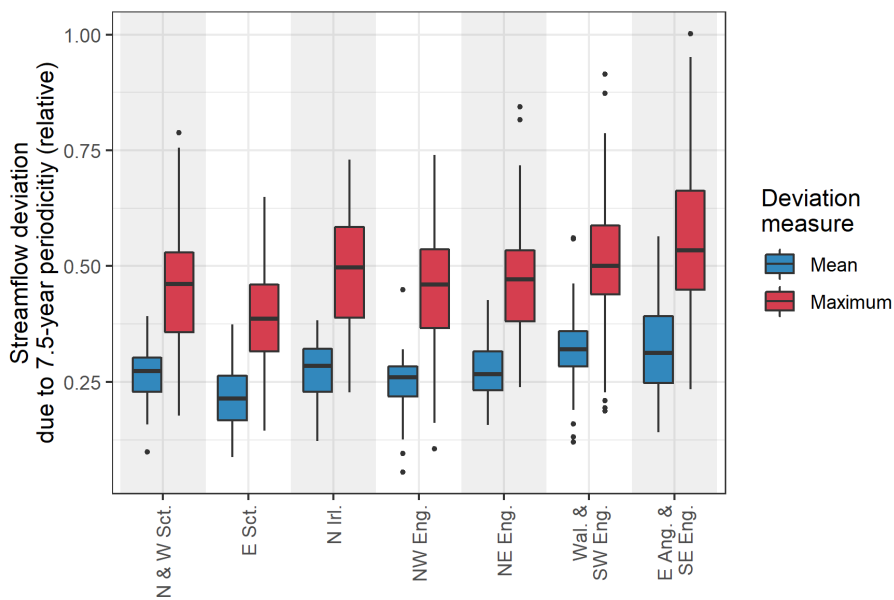
451

452



453

454 Figure 6 – Distribution of absolute mean and maximum modulation of summer groundwater  
455 level as a result of the principal cross-wavelet periodicity between the NAOI and winter  
456 Groundwater level by aquifer region



457





458 Figure 7 – Modulation of summer streamflow (relative to record standard deviation) as a  
459 result of the principal cross-wavelet periodicity between the NAOI and winter streamflow.

## 460 5. Discussion

### 461 5.1. Historical covariances between the NAOI and water resources at multiannual 462 periodicities

463 Our results show that the dominant mode of multiannual covariance between the NAOI and  
464 UK water resources is at the ~7.5-year periodicity. This is apparent in the time-averaged  
465 covariance significance plots for groundwater (figure 2b) and streamflow (figure 3b). The  
466 same 7.5-year periodicity is also the strongest average mode of periodic behaviour in water  
467 resource extremes. Periodicities of similar lengths have previously been detected in  
468 European GWL records, such as those in the UK (Rust et al, 2018 Holman et al, 2011),  
469 Hungary (Garamhegyi et al, 2016), Spain (Luque-Espinar et al, 2008), Italy (De Vita et al  
470 2011), and Germany (Liesch and Wunsch, 2019); and European streamflow records, for  
471 example in the UK (Rust et al 2021; Burt and Howden, 2013) and Sweden (Uvo et al, 2021).  
472 Our results therefore are consistent with principal periodicities detected in wider European  
473 water resources and highlight the NAO's wide-scale control on water resource extremes.

474 Despite the prominence of the average 7.5-year periodicity in water resource variables, the  
475 wider time-frequency spectra show that the NAO's multiannual control on water resources is  
476 subject to considerable transience and non-stationarity across time and frequency. For  
477 instance, the percentage of water resource records with a significant covariance with the  
478 NAOI at the 7.5-year periodicity remains below 10% until between 1960 and 1965, with  
479 significance becoming abruptly widespread (> 30%) between 1980 and 1985. As such this  
480 suggests that the NAO's control on water resources, at the 7.5-year periodicity, has only  
481 been prominent over the past four to five decades. Furthermore, prior to this mode of  
482 behaviour, an approximate 16-year periodicity predominated the water resource extremes  
483 record that did not covary with NAOI. Previous studies have associated a minimum in this  
484 16-year cycle in water resources with the wide-scale 1976 drought (Rust et al, 2019) that



485 affected most UK water resources, particularly in the south of the country (Rodda and  
486 Marsh, 2011). These findings are also consistent with Barker et al (2019) who demonstrate  
487 longer duration drought events in the UK for the period 1940 to 1980 (approximately), and  
488 comparatively shorter drought durations for the period 1980 to present. This may be  
489 explained by a more prominent low-frequency influence on water resources and extremes  
490 during this former period (1940 – 1980), causing longer negative anomalies on drought  
491 indices. Finally, Holman et al (2011) linked a 16-year periodic behaviour in groundwater  
492 records with the East Atlantic pattern, the second-most dominant mode of atmospheric  
493 variability in the North Atlantic region. Our results could be interpreted as suggesting an  
494 abrupt shift towards increased frequency of water resource extremes around 1970 to 1980  
495 as a result of a transition of periodic control from the EA to the NAO. This interpretation may  
496 expand on findings from Neves et al (2019) who demonstrate that historical droughts in  
497 southwest Europe are better explained with a combination of NAO and EA influence.

498

499 Multiple studies have noted a marked change in European hydrological drought trends since  
500 the 1970s, often in the context of the ongoing effects of climate change on water resources  
501 (Tanguy et al 2021; Rodda and Marsh, 2011; Bloomfield et al., 2019). These impacts vary  
502 depending on the water resource and region but can include changing drought frequency  
503 (Spinoni et al, 2015; Bloomfield et al., 2019; Chiang et al, 2021), severity (Hanel et al, 2018;  
504 Bloomfield et al., 2019), and increasing divergence of drought characteristic across Europe  
505 (Cammalleri et al, 2020). We show here that a dominant 7.5-year periodicity, driven by the  
506 NAO, has occurred coincident to these reported changing trends, and proceeded a  
507 secondary periodicity of approximately 16 years. As such our results suggest that some of  
508 the change in drought frequency that has been noted to have occurred since the 1970s, may  
509 be in-part driven by the NAO's increased periodic control on water resources. Hydroclimate  
510 studies often highlight that the interaction between climate change, ocean-atmosphere  
511 processes and land-surface processes may be complex, resulting in non-linear hydrological



512 responses to increasing global temperatures (Rial et al 2004, Wu et al, 2018). As such, the  
513 abrupt emergence of a 7.5-year periodicity between the NAO and water resource extremes  
514 between 1980 and 1985, and its weakening since 2005, may be evidence of this type of non-  
515 linear response. While there have been many studies assessing the impact of climate  
516 change projections on the NAO (e.g. Rind et al (2005); Woolings and Blackburn (2012)),  
517 there have been few that have investigated potential interactions between climate change  
518 and multiannual periodicities in the NAO. As such, the role of climate change in affecting the  
519 non-stationary periodicities (detected in this study) is currently unknown.

520 Yuan et al (2017) highlight the importance of suitable calibration period selection for the  
521 development of drought early warning systems, particularly in climate change scenarios.  
522 Many of these systems in Europe (e.g. Hall and Hanna, 2018; Svensson et al., 2015) rely on  
523 high-resolution hydrometeorological datasets for calibration of historical relationships, many  
524 of which are only available for recent decades (Rust et al, 2021b, Sun et al 2018). We show  
525 here that frequency statistics potentially used as calibration bases for water resource early  
526 warning systems can exhibit both multidecadal periods of stability and abrupt sub-decadal  
527 non-stationarities, driven by multiannual behaviours in the NAO. Furthermore, we show a  
528 weakening of the dominant 7.5-year periodicity since 2005, suggesting a different frequency  
529 structure may predominate water resource extremes from the 2020s. This further highlights  
530 the need for continuous recalibration of critical forecasting utilities, and the potential benefit  
531 of including the NAOI as a covariate when understanding multiannual periodic variability in  
532 European water resources.

533



534 **5.2. Phase difference between NAO and water resource records at 7.5-year**  
535 **periodicity**

536 The quantification of lead times between meteorological processes and water resource  
537 response is critical in the development of early warning systems for water resource  
538 management. As such, hydroclimate studies have sought to investigate temporal lags  
539 between multiannual periodicities in the NAO and water resource variables across Europe  
540 (Uvo et al, 2021, Neves et al 2019, Holman et al 2011). However, previous research has  
541 highlighted that the relationship strength and sign between the NAO and European rainfall is  
542 non-stationary at sub-decadal to decadal timescales (Rust et al 2021, Vicente-Serrano &  
543 López-Moreno, 2008). The extent to which this non-stationarity is projected to multiannual  
544 periodicities in water resources was previously unknown. Sign change is synonymous with a  
545 phase difference shift of approximately  $\pi$  between periodic components of the NAO and  
546 water resources, and as such has the potential to disrupt the projection of lead times into  
547 future scenarios. Here we assess the phase difference between the NAO and water  
548 resources at a country scale to identify the extent to which this non-stationary is present at  
549 multiannual periodicities.

550 Most water resources records exhibit an abrupt shift in phase difference of approximately  $-\pi$   
551 around 1990. An earlier shift (of approximately  $+\pi$ ) is also apparent between 1970 and 1980,  
552 however this is less temporally aligned across the fewer records that cover this period. This  
553 suggests that, for the period of approximately 1970 to 1990, the relationship sign between  
554 the NAO and water resources was inverted. Furthermore, the timing of this period of  
555 inversion generally aligns with reported periods of sign inversion in existing studies between  
556 the NAO and UK rainfall (Rust et al 2021, Vicente-Serrano & López-Moreno, 2008). It is  
557 interesting to note that this period of inversion is notably shorter for some groundwater level  
558 records of the Chalk (e.g., those in South Chalk and Thames and Chiltern Chalk). Rust et al  
559 (2021) showed the south and south east of the UK was subject to the increased non-  
560 stationarity of the NAO-precipitation relationship when compared to other regions, which



561 may explain these relatively short periods of relationship inversion. A similar spatial pattern  
562 is shown in the streamflow records, with minimal phase difference shifts in northwest  
563 England, Scotland, and Northern Ireland where more stable signs have been found by Rust  
564 et al (2021b).

565 Localisation of this non-stationarity between the NAO and water resources at multiannual  
566 periodicities suggests it is possible to identify a discrete time period of sufficient stationarity  
567 from which to calculate lead-in times for early warning systems (for instance, between 1990  
568 and 2020). However, phase differences for this period also show a degree of non-  
569 stationarity, varying by up to approximately  $\pm\frac{1}{4}\pi$ . Some of this variance may be due to  
570 changing storage dynamics within a catchment over time (Rust et al, 2014; Beverly and  
571 Hocking, 2012), but also the introduction of red noise from reconstructing from non-  
572 significant wavelets. This also explains the increased variance seen in aquifer groups  
573 characterised by higher autocorrelation (e.g., Sandstone) (Bloomfield and Marchant, 2013),  
574 and the relatively low variance seen in streamflow records which often have lower  
575 autocorrelation when compared to groundwater level (Hannaford et al, 2021). While this  
576 can be minimised by calculating phase difference from significant wavelets only, we have  
577 shown in the previous section that the significance between the NAO and water resources  
578 and multiannual periodicities is also subject to notable non-stationarity.

579 Finally, in order to calculate accurate lead-in times between periodicities in the NAO and  
580 water resources in future scenarios, a sufficient systematic understanding of the NAO sign  
581 non-stationarity is required. However, there is limited research that has investigated the  
582 causes for these modes of multiannual non-stationarity. Vicente-Serrano & López-  
583 Moreno (2008) suggest that an eastward shift of the NAO's southern centre of action may  
584 account for a portion of this variability, but highlight that further work is required for this to be  
585 a sufficient explanation of a changing correlation between the NAO and European rainfall.  
586 As such, existing non-stationarities between the NAO and water resources at multiannual



587 periodicities remains a considerable barrier to its application in improving preparedness for  
588 future water resource extremes.

### 589 **5.3. NAO multiannual modulations on water resources in future scenarios**

590 Water resource management systems are in place across Europe to improve planning and  
591 preparedness for the projected effects of climate change. As such, in order for multiannual  
592 NAO modulations of water resources to have sufficient utility for water management systems  
593 in future scenarios, they need to exhibit a comparable influence on water resources to the  
594 projected effects of climate change. Here, we present historical modulations of summer  
595 water resource variables from the principal NAO periodicity alongside expected impacts on  
596 water resources from climate change projections in order to discuss their comparative  
597 influence.

598 Jackson et al (2015) estimated median groundwater level change due to climate change in  
599 24 boreholes across Chalk, limestone, sandstone and greensand aquifer groups in the UK  
600 for the 2050s under a high emission scenario for September (as a typical annual minima of  
601 groundwater levels in the UK). Median level from each site in Jackson et al (2015) have  
602 been regrouped and averaged across the broad aquifer groups used in this study to allow  
603 comparison with historical deviations in water resource results as a result of the NAO's 7.5-  
604 year periodicity. This comparison is provided in Table 1. A mapping table of this comparison  
605 is available in the supplementary material.

606



Aquifer group	50 <sup>th</sup> %ile gwI change due to climate change ( m)	Gwl deviation due to 7.5-year NAO periodicity (± m) (med.mean)	Gwl deviation due to 7.5-year NAO periodicity (± m) (med.max)
Chalk (East Anglia)	-0.21	0.16	0.31
Chalk (Lincolnshire)	-0.31	0.71	1.03
Chalk (South)	-0.64	0.73	1.08
Chalk (Thames / Chilterns)	-0.69	0.86	1.33
Limestone	-0.28	0.35	0.51
Oolite	-0.36	0.21	0.33
Sandstone	-0.07	0.15	0.25
Greensands	-0.10	0.12	0.17

607 Table 1 – synthesis of Table 3 from Jackson et al (2015). Median results from the absolute  
 608 teleconnection modulation on groundwater level from Figure 3 of this paper are also  
 609 presented for the mean and maximum modulation cases. NAO teleconnection modulations  
 610 greater than the reported 50<sup>th</sup> percentile climate change modulation are shaded in grey.

611  
 612  
 613 Historical modulations in groundwater level due to multiannual periodicities in the NAO were  
 614 greater than projected GWL modulation from a high emissions climate change scenario, in  
 615 all but two aquifer groups for mean NAO modulation (East Anglia Chalk, Oolite), and all but  
 616 one for maximum NAO modulation (Oolite). Similar degrees of GWL modulation from climate  
 617 change scenarios have been shown for wider European aquifer systems (e.g., Dams et al,  
 618 2011), and our results for NAO modulations of GWL are of a similar degree to those reported  
 619 by Neves et al (2019) for aquifers in the Iberian Peninsula. While few studies have looked at  
 620 multiannual NAO modulations of groundwater level across Europe, our results here suggest  
 621 a similar response across Western Europe, where the NAO has a greater influence on  
 622 precipitation (Trigo et al, 2002). However, existing studies notable uncertainties in the future  
 623 trends of groundwater level change due to climate change. For instance, Yusoff et al. (2002)  
 624 demonstrated that it was not possible to predict whether groundwater level would rise or fall  
 625 between 2020s and 2050s, Bloomfield et al. (2003) showed that groundwater levels were  
 626 expected to rise in the 2020s but fall in the 2050s, and, Jackson et al (2015) showed



627 reductions in annual and average summer levels but increases in average winter levels by  
628 the 2050s. For streamflow, Kay et al (2020) give estimated modulations to low flows (Q95)  
629 as a result of climate change (2050 horizon). While no Scottish catchments were used in the  
630 study, percentage modulations for low flows were found to be mostly between 0 to -20%  
631 change with some catchments showing up to -40% change for catchments in the West and  
632 South West of the UK. Schnieder et al (2013) show similar low flow modulations across  
633 Europe as a result of climate change, ranging from +20% for northwest Europe to -40% in  
634 the Iberian Peninsula. As such, our results for streamflow (Figure 7) indicate that multiannual  
635 NAO modulation of streamflow has been, on average, comparable to the expected change  
636 due to climate change scenarios. NAO modulations in streamflow are notably less than  
637 those found in groundwater level, as may be expected given the established sensitivity of  
638 groundwater processes to long-term changes in meteorological fluxes (Forootan et al., 2018;  
639 Van Loon, 2015; Folland et al., 2015).

640 Given the scale of multiannual NAO influence on water resource compared to the estimated  
641 effects of climate change, the NAO may have the potential to impact the projected trend of  
642 water resource variability in certain future scenarios more than was previously understood,  
643 and therefore effect the required adaptive management response. However, existing  
644 research has shown that that current GCMs do not fully replicate low frequency behaviours  
645 in the NAO that have been historical recorded (Eade et al, 2021). Given the importance of  
646 multiannual periodicities the NAO in defining water resource behaviour, demonstrated here  
647 and in other research (e.g., Uvo et al, 2021; Neves et al, 2019), this raises notable  
648 uncertainties in the use of GCMs outputs for projecting European water resource behaviour  
649 into future scenarios. Findings reported here suggest that current projections from these  
650 GCMs may contain error that is comparable to the current projected effect of climate change  
651 on water resources. This therefore highlights the need for improved low frequency  
652 representation in GCMs, and for an understanding of the non-stationary atmospheric  
653 behaviours are can considerably influence wide-scale water resource behaviour.





654 Rust et al (2018) set out a conceptual model for how multiannual modulations of water  
655 resources due to the NAO may provide a system for improving water resource forecasts and  
656 management regimes. This model highlights the need for a systematic understanding of how  
657 multiannual periodicities affect water resources over time, including temporal lags and  
658 amplitude modulation between the NAO and water resources. We demonstrate that the  
659 degree to which the NAO's 7.5-year periodicity has modulated historical water resources is  
660 of a similar order of magnitude to the estimated impacts on water resource variables from  
661 climate change projections. These results further show the importance of including the  
662 influence of multiannual NAO periodicities on water resources in the understanding of future  
663 extremes, as they have the potential to affect the required management regime for certain  
664 resources in climate change scenarios. However, we also show that there are notable non-  
665 stationarities in NAO periodicities over time and their relationship with water resource  
666 response, for which there is limited systematic understanding in existing hydroclimate  
667 literature.

668

## 669 **6. Conclusions**

670 This paper assesses the utility of the relationship between the NAO and water resources, at  
671 multiannual periodicities, for improving preparedness of water resource extremes in Europe.  
672 We review this relationship in the context of non-stationary dynamics within the NAO and its  
673 control on UK meteorological variables, as well as its potential impact on water resources in  
674 climate change scenarios. We provide new evidence for the time-frequency relationship  
675 between the NAO and water resources in western Europe showing that a wide-spread 7.5-  
676 year periodicity, which predominates the multiannual frequency structure of many European  
677 water resources, is the result of a non-stationary control from the NAO between  
678 approximately 1970 and 2020. Furthermore, we show that known non-stationarities of the  
679 relationship sign between the NAOI and European rainfall at the annual scale are present in  
680 water resources at multiannual scales. A current lack of systematic understanding of both



681 these forms of non-stationarity, in existing atmospheric or meteorological literature, is a  
682 considerable barrier to the application of this multiannual relationship for improving  
683 preparedness for future water resource extremes. However, we also show that the degree of  
684 modulation from multiannual NAO periodicities on water resources can be comparable to  
685 modulations from a worst-case climate change scenario. As such multiannual periodicities  
686 offer a valuable explanatory variable for ongoing water resource behaviour that have the  
687 potential to heavily impact the required management regimes for individual resources in  
688 climate change scenarios. Therefore, we highlight knowledge gaps in atmospheric research  
689 (e.g. the ability of climate models to simulate NAO non-stationarities) that need to be  
690 addressed in order for multiannual NAO periodicities to be used in improving early warning  
691 systems or improving preparedness for water resource extremes.

692 **Data availability.**

693 The groundwater level data used in the study are from the WellMaster Database in the  
694 National Groundwater Level Archive of the British Geological Survey. The data are available  
695 under license from the British Geological Survey at <https://www.bgs.ac.uk/products/hydrogeology/WellMaster.html> (last accessed: 24/10/2021).

697 The streamflow data as well as the metadata used in this study are freely available at the  
698 NRFA website at <http://nrfa.ceh.ac.uk/> (last accessed: 25/10/2021).

699 The data that support the findings of this study are available in CORD at  
700 10.17862/cranfield.rd.16866868. This study was a re-analysis of existing data that are  
701 publicly available from NCAR at <https://climatedataguide.ucar.edu/climate-data>.

702

703 **Author contributions.**

704 WR designed the methodology and carried them out with supervision from all co-authors. WR  
705 prepared the article with contributions from all co-authors.



706 **Competing interests.**

707 The authors declare that they have no conflict of interest.

708

709 **Acknowledgements.**

710 This work was supported by the Natural Environment Research Council (grant numbers  
711 NE/M009009/1 and NE/L010070/1) and the British Geological Survey (Natural Environment  
712 Research Council). JPB publishes with the permission of the Executive Director, British  
713 Geological Survey (NERC). MOC gratefully acknowledges funding for an Independent  
714 Research Fellowship from the UK Natural Environment Research Council (NE/P017819/1).  
715 We thank Angi Rosch and Harald Schmidbauer for making their wavelet package  
716 “WaveletComp” freely available.

717

718 **Financial support.**

719 This research has been supported by the Natural Environment Research Council (grant nos.  
720 NE/M009009/1 and NE/L010070/1), and MOC has been supported by an Independent  
721 Research Fellowship from the UK Natural Environment Research Council (NE/P017819/1).

722

723 **References**

724 Allen, D.J., Brewerton, L.J., Coleby, L.M., Gibbs, B.R., Lewis, M.A., MacDonald, A.M.,  
725 Wagstaff, S.J., Williams, A.T.: The physical properties of major aquifers in England and  
726 Wales. British Geological Survey, 333pp, BGS Report WD/97/034,  
727 <http://nora.nerc.ac.uk/id/eprint/13137/>, 1997,



- 728 Allen, M. R., Smith, L. A., Allen, M. R., and Smith, L. A.: Monte Carlo SSA: Detecting  
729 irregular oscillations in the Presence of Colored Noise, *J. Clim.*, 9, 3373–3404,  
730 [https://doi.org/10.1175/1520-0442\(1996\)009<3373:MCSPIO>2.0.CO;2](https://doi.org/10.1175/1520-0442(1996)009<3373:MCSPIO>2.0.CO;2), 1996.
- 731 Beverly, C. and Hocking, M.: Predicting Groundwater Response Times and Catchment  
732 Impacts From Land Use Change, *Australasian Journal of Water Resources*, 16, 29–47,  
733 <https://doi.org/10.7158/13241583.2012.11465402>, 2012.
- 734 Bloomfield, J.P.: The role of diagenesis in the hydrogeological stratification of carbonate  
735 aquifers: An example from the Chalk at Fair Cross, Berkshire, UK, *Hydrol. Earth Syst. Sci.*,  
736 1, 19-33, <https://doi.org/10.5194/hess-1-19-1997>, 1997.
- 737 Bloomfield, J. P., Gaus, I., and Wade, S. D.: A method for investigating the potential impacts  
738 of climate-change scenarios on annual minimum groundwater levels,  
739 <https://doi.org/10.1111/j.1747-6593.2003.tb00439.x>, 2003.
- 740 Bloomfield, J. P. and Marchant, B. P.: Analysis of groundwater drought building on the  
741 standardised precipitation index approach, *Hydrol. Earth Syst. Sci.*, 17, 4769–4787,  
742 <https://doi.org/10.5194/hess-17-4769-2013>, 2013.
- 743 Bloomfield, J.P., Marchant, B.J., and McKenzie, A.A.: 2019. Changes in groundwater drought  
744 associated with anthropogenic warming, *Hydrol. Earth Syst. Sci.*, 23, 1393–1408,  
745 <https://doi.org/10.5194/hess-23-1393-2019>, 2019.
- 746 Bonaccorso, B., Cancelliere, A., and Rossi, G.: Probabilistic forecasting of drought class  
747 transitions in Sicily (Italy) using Standardized Precipitation Index and North Atlantic  
748 Oscillation Index, *J. Hydrol.*, 526, 136–150, <http://dx.doi.org/10.1016/j.jhydrol.2015.01.070>,  
749 2015
- 750 Brady, A., Faraway, J., and Prosdociimi, I.: Attribution of long-term changes in peak river  
751 flows in Great Britain, *Hydrol. Sci. J.*, 64, 1159–1170,  
752 <https://doi.org/10.1080/02626667.2019.1628964>, 2019.



- 753 Burt, T. P. and Howden, N. J. K.: North Atlantic Oscillation amplifies orographic precipitation  
754 and river flow in upland Britain, *Water Resour. Res.*, 49, <https://doi.org/10.1002/wrcr.20297>,  
755 2013.
- 756 Cammalleri, C., Naumann, G., Mentaschi, L., Bisselink, B., Gelati, E., De Roo, A., and  
757 Feyen, L.: Diverging hydrological drought traits over Europe with global warming, *Hydrol.*  
758 *Earth Syst. Sci.*, 24, 5919–5935, <https://doi.org/10.5194/hess-24-5919-2020>, 2020.
- 759 Chiang, F., Mazdiyasn, O., and AghaKouchak, A.: Evidence of anthropogenic impacts on  
760 global drought frequency, duration, and intensity, *Nat. Commun.*, 12, 2754,  
761 <https://doi.org/10.1038/s41467-021-22314-w>, 2021.
- 762 Coleman, J. S. M. and Budikova, D.: Eastern U.S. summer streamflow during extreme  
763 phases of the North Atlantic oscillation, *J. Geophys. Res.*, 118, 4181–4193,  
764 <http://dx.doi.org/10.1002/jgrd.50326>, 2013.
- 765 Dams, J., Salvatore, E., Van Daele, T., Ntegeka, V., Willems, P., and Batelaan, O.: Spatio-  
766 temporal impact of climate change on the groundwater system, *Hydrol. Earth Syst. Sci.*, 16,  
767 1517–1531, <https://doi.org/10.5194/hess-16-1517-2012>, 2012.
- 768 Deser, C., Hurrell, J. W., and Phillips, A. S.: The role of the North Atlantic Oscillation in  
769 European climate projections, *Clim. Dyn.*, 49, 3141–3157, [https://doi.org/10.1007/s00382-](https://doi.org/10.1007/s00382-016-3502-z)  
770 016-3502-z, 2017.
- 771 De Vita, P., Allocca, V., Manna, F., and Fabbrocino, S.: Coupled decadal variability of the  
772 North Atlantic Oscillation, regional rainfall and karst spring discharges in the Campania  
773 region (southern Italy), *Hydrol. Earth Syst. Sci.*, 16, 1389–1399, [https://doi.org/10.5194/hess-](https://doi.org/10.5194/hess-16-1389-2012)  
774 16-1389-2012, 2012.
- 775 Dixon, H., Hannaford, J., and Fry, M. J. The effective management of national hydrometric  
776 data: experiences from the United Kingdom, *Hydrological Sciences Journal*, 58:7, 1383-  
777 1399, DOI: 10.1080/02626667.2013.787486. 2013



- 778 Feng, P.-N., Lin, H., Derome, J., and Merlis, T. M.: Forecast Skill of the NAO in the  
779 Subseasonal-to-Seasonal Prediction Models, *J. Clim.*, 34, 4757–4769,  
780 <https://doi.org/10.1175/JCLI-D-20-0430.1>, 2021.
- 781 Folland, C. K., Hannaford, J., Bloomfield, J. P., Kendon, M., Svensson, C., Marchant, B. P.,  
782 Prior, J., and Wallace, E.: Multi-annual droughts in the English Lowlands: a review of their  
783 characteristics and climate drivers in the winter half-year, *Hydrol. Earth Syst. Sci.*, 19, 2353–  
784 2375, <https://doi.org/10.5194/hess-19-2353-2015>, 2015.
- 785 Forootan, E., Khaki, M., Schumacher, M., Wulfmeyer, V., Mehrnegar, N., van Dijk, A. I. J. M.,  
786 Brocca, L., Farzaneh, S., Akinluyi, F., Ramillien, G., Shum, C. K., Awange, J., and  
787 Mostafaie, A.: Understanding the global hydrological droughts of 2003–2016 and their  
788 relationships with teleconnections, *Sci. Total Environ.*,  
789 <https://doi.org/10.1016/J.SCITOTENV.2018.09.231>, 2018.
- 790 Gao, L., Deng, Y., Yan, X., Li, Q., Zhang, Y., and Gou, X.: The unusual recent streamflow  
791 declines in the Bailong River, north-central China, from a multi-century perspective, *Quat.*  
792 *Sci. Rev.*, 260, 106927, <http://dx.doi.org/10.1016/j.quascirev.2021.106927>, 2021.
- 793 Garamhegyi, T., Kovács, J., Pongrácz, R., Tanos, P., and Hatvani, I. G.: Investigation of the  
794 climate-driven periodicity of shallow groundwater level fluctuations in a Central-Eastern  
795 European agricultural region, *Hydrogeol. J.*, 26, 677–688, [https://doi.org/10.1007/s10040-](https://doi.org/10.1007/s10040-017-1665-2)  
796 017-1665-2, 2018.
- 797 Hanel, M., Rakovec, O., Markonis, Y., Máca, P., Samaniego, L., Kyselý, J., and Kumar, R.:  
798 Revisiting the recent European droughts from a long-term perspective, *Sci. Rep.*, 8, 9499,  
799 <https://doi.org/10.1038/s41598-018-27464-4>, 2018.
- 800 Holman, I., Rivas-Casado, M., Bloomfield, J. P., and Gurdak, J. J.: Identifying non-stationary  
801 groundwater level response to North Atlantic ocean-atmosphere teleconnection patterns  
802 using wavelet coherence, *Hydrogeol. J.*, 19, 1269–1278, [https://doi.org/10.1007/s10040-](https://doi.org/10.1007/s10040-011-0755-9)  
803 011-0755-9, 2011.



- 804 Hurrell, J. W., Kushnir, Y., Ottersen, G., and Visbeck, M.: An Overview of the North Atlantic  
805 Oscillation, in: The North Atlantic Oscillation: Climatic Significance and Environmental  
806 Impact, American Geophysical Union, 1–35, <https://doi.org/10.1029/GM134> 2003.
- 807 Hurrell, J. W.: Decadal trends in the north atlantic oscillation: regional temperatures and  
808 precipitation, *Science*, 269, 676–679, <https://doi.org/10.1126/science.269.5224.676>, 1995.
- 809 Hurrell, J. W. and Deser, C.: North Atlantic climate variability: The role of the North Atlantic  
810 Oscillation, *J. Mar. Syst.*, 79, 231–244, <https://doi.org/10.1016/j.jmarsys.2008.11.026>, 2010.
- 811 Jackson, C. R., Bloomfield, J. P., and Mackay, J. D.: Evidence for changes in historic and  
812 future groundwater levels in the UK, *Prog. Phys. Geogr.*, 39, 49–67,  
813 <https://doi.org/10.1177%2F0309133314550668>, 2015.
- 814 Kay, A. L., Watts, G., Wells, S. C., and Allen, S.: The impact of climate change on U. K. river  
815 flows: A preliminary comparison of two generations of probabilistic climate projections,  
816 *Hydrol. Process.*, 34, 1081–1088, <https://doi.org/10.1002/hyp.13644>, 2020.
- 817 Konapala, G., Mishra, A. K., Wada, Y., and Mann, M. E.: Climate change will affect global  
818 water availability through compounding changes in seasonal precipitation and evaporation,  
819 *Nat. Commun.*, 11, 3044, <https://doi.org/10.1038/s41467-020-16757-w>, 2020.
- 820 Kingston, D. G., McGregor, G. R., Hannah, D. M., and Lawler, D. M.: River flow  
821 teleconnections across the northern North Atlantic region, *Geophys. Res. Lett.*, 33, 1–5,  
822 <http://dx.doi.org/10.1029/2006GL026574>, 2006.
- 823 Kuss, A. M. and Gurdak, J. J.: Groundwater level response in U.S. principal aquifers to  
824 ENSO, NAO, PDO, and AMO, *J. Hydrol.*, 519, 1939–1952,  
825 <https://doi.org/10.1016/j.jhydrol.2014.09.069>, 2014.
- 826 Labat, D.: Cross wavelet analyses of annual continental freshwater discharge and selected  
827 climate indices, *J. Hydrol.*, 385, 269–278, <https://doi.org/10.1016/j.jhydrol.2010.02.029>,  
828 2010.



- 829 Liesch, T. and Wunsch, A.: Aquifer responses to long-term climatic periodicities, *J. Hydrol.*,  
830 572, 226–242, <http://dx.doi.org/10.1016/j.jhydrol.2019.02.060>, 2019.
- 831 Luque-Espinar, J. A., Chica-Olmo, M., Pardo-Igúzquiza, E., and García-Soldado, M. J.:  
832 Influence of climatological cycles on hydraulic heads across a Spanish aquifer, *J. Hydrol.*,  
833 354, 33–52, <https://doi.org/10.1016/j.jhydrol.2008.02.014>, 2008.
- 834 Marchant, B.P., and Bloomfield, J.P.: Spatio-temporal modelling of the status of groundwater  
835 droughts, *J. Hydrol.*, 564, 397-413, <https://doi.org/10.1016/j.jhydrol.2018.07.009>, 2018.
- 836 Marsh, T. and Hannaford, J.: UK Hydrometric Register. Hydrological data UK series, Centre  
837 for Ecology and Hydrology, 2008.
- 838 Meinke, H., deVoil, P., Hammer, G. L., Power, S., Allan, R., Stone, R. C., Folland, C., and  
839 Potgieter, A.: Rainfall variability of decadal and longer time scales: Signal or noise?, *J. Clim.*,  
840 18, 89–90, <https://doi.org/10.1175/JCLI-3263.1>, 2005.
- 841 Naumann, G., Spinoni, J., Vogt, J. V., and Barbosa, P.: Assessment of drought damages  
842 and their uncertainties in Europe, *Environ. Res. Lett.*, 10, 124013,  
843 <http://dx.doi.org/10.1088/1748-9326/10/12/124013>, 2015.
- 844 Neves, M. C., Jerez, S., and Trigo, R. M.: The response of piezometric levels in Portugal to  
845 NAO, EA, and SCAND climate patterns, *J. Hydrol.*, 568, 1105–1117,  
846 <http://dx.doi.org/10.1016/j.jhydrol.2018.11.054>, 2019.
- 847 Rial, J. A., Pielke, R. A., Sr, Beniston, M., Claussen, M., Canadell, J., Cox, P., Held, H., de  
848 Noblet-Ducoudré, N., Prinn, R., Reynolds, J. F., and Salas, J. D.: Nonlinearities, feedbacks  
849 and critical thresholds within the earth's climate system, *Clim. Change*, 65, 11–38,  
850 <https://doi.org/10.1023/B:CLIM.0000037493.89489.3f>, 2004.
- 851 Rodda, J. and Marsh, T.: The 1975-76 Drought - a contemporary and retrospective review,  
852 Centre for Ecology & Hydrology, 2011.





- 853 Rosch, A. and Schmidbauer, H.: WaveletComp 1.1: a guided tour through the R package,  
854 2018.
- 855 Rust, W., Bloomfield, J. P., Cuthbert, M. O., Corstanje, R., and Holman, I. P.: Non-stationary  
856 control of the NAO on European rainfall and its implications for water resource management,  
857 *Hydrol. Process.*, 35, <https://doi.org/10.1002/hyp.14099>, 2021b.
- 858 Rust, W., Corstanje, R., Holman, I. P., and Milne, A. E.: Detecting land use and land  
859 management influences on catchment hydrology by modelling and wavelets, *J. Hydrol.*, 517,  
860 378–389, 2014.
- 861 Rust, W., Cuthbert, M., Bloomfield, J., Corstanje, R., Howden, N., and Holman, I.: Exploring  
862 the role of hydrological pathways in modulating multi-annual climate teleconnection  
863 periodicities from UK rainfall to streamflow, *Hydrol. Earth Syst. Sci.*, 25, 2223–2237,  
864 <https://doi.org/10.1016/j.jhydrol.2014.05.052>, 2021a.
- 865 Rust, W., Holman, I., Bloomfield, J., Cuthbert, M., and Corstanje, R.: Understanding the  
866 potential of climate teleconnections to project future groundwater drought, *Hydrol. Earth  
867 Syst. Sci.*, 23, 3233–3245, <https://doi.org/10.5194/hess-23-3233-2019>, 2019.
- 868 Rust, W., Holman, I., Corstanje, R., Bloomfield, J., and Cuthbert, M.: A conceptual model for  
869 climatic teleconnection signal control on groundwater variability in Europe, *Earth-Sci. Rev.*,  
870 177, 164–174, <https://doi.org/10.1016/j.earscirev.2017.09.017>, 2018.
- 871 Sang, Y.-F.: A review on the applications of wavelet transform in hydrology time series  
872 analysis, *Atmos. Res.*, 122, 8–15, <https://doi.org/10.1016/j.atmosres.2012.11.003>, 2013.
- 873 Schneider, C., Laizé, C. L. R., Acreman, M. C., and Flörke, M.: How will climate change  
874 modify river flow regimes in Europe?, *Hydrol. Earth Syst. Sci.*, 17, 325–339,  
875 <https://doi.org/10.5194/hess-17-325-2013>, 2013.



- 876 Sun, Q., Miao, C., Duan, Q., Ashouri, H., Sorooshian, S., and Hsu, K.: A review of global  
877 precipitation data sets: Data sources, estimation, and intercomparisons, *Rev. Geophys.*, 56,  
878 79–107, <https://doi.org/10.1002/2017RG000574>, 2018.
- 879 Sutanto, S. J., Van Lanen, H. A. J., Wetterhall, F., and Lloret, X.: Potential of Pan-European  
880 Seasonal Hydrometeorological Drought Forecasts Obtained from a Multihazard Early  
881 Warning System, *Bull. Am. Meteorol. Soc.*, 101, E368–E393, [https://doi.org/10.1175/BAMS-](https://doi.org/10.1175/BAMS-D-18-0196.1)  
882 [D-18-0196.1](https://doi.org/10.1175/BAMS-D-18-0196.1), 2020.
- 883 Svensson, C., Brookshaw, A., Scaife, A. A., Bell, V. A., Mackay, J. D., Jackson, C. R.,  
884 Hannaford, J., Davies, H. N., Arribas, A., and Stanley, S.: Long-range forecasts of UK winter  
885 hydrology, *Environ. Res. Lett.*, 10, 064006, <http://dx.doi.org/10.1088/1748-9326/10/6/064006>  
886 2015.
- 887 Tremblay, L., Larocque, M., Anctil, F., and Rivard, C.: Teleconnections and interannual  
888 variability in Canadian groundwater levels, *J. Hydrol.*, 410, 178–188,  
889 <https://doi.org/10.1016/j.jhydrol.2011.09.013>, 2011.
- 890 Trigo, R. M., Osborn, T. J., and Corte-real, J. M.: The North Atlantic Oscillation influence on  
891 Europe: climate impacts and associated physical mechanisms, *Clim. Res.*, 20, 9–17,  
892 <http://dx.doi.org/10.3354/cr020009>, 2002.
- 893 Tanguy, M., Haslinger, K., Svensson, C., Parry, S., Barker, L. J., Hannaford, J., and  
894 Prudhomme, C.: Regional Differences in Spatiotemporal Drought Characteristics in Great  
895 Britain, *Front. Environ. Sci. Eng. China*, 9, 67, <https://doi.org/10.3389/fenvs.2021.639649>,  
896 2021.
- 897 Uvo, C. B., Foster, K., and Olsson, J.: The spatio-temporal influence of atmospheric  
898 teleconnection patterns on hydrology in Sweden, 34, 100782,  
899 <http://dx.doi.org/10.1016/j.ejrh.2021.100782>, 2021.



- 900 Velasco, E. M., Gurdak, J. J., Dickinson, J. E., Ferré, T. P. A., and Corona, C. R.:  
901 Interannual to multidecadal climate forcings on groundwater resources of the U.S. West  
902 Coast, <https://doi.org/10.1016/j.ejrh.2015.11.018>, 2015.
- 903 Van Loon, A.F. On the propagation of drought: How climate and catchment characteristics  
904 influence hydrological drought development and recovery. PhD thesis Wageningen  
905 University. 2013.
- 906 Vicente-Serrano, S. M. and López-Moreno, J. I.: Differences in the non-stationary influence  
907 of the North Atlantic Oscillation on European precipitation under different scenarios of  
908 greenhouse gas concentrations, <https://doi.org/10.1029/2008gl034832>, 2008.
- 909 Van Loon, A. F.: Hydrological drought explained, *WIREs Water*, 2, 359–392,  
910 <https://doi.org/10.1002/wat2.1085>, 2015.
- 911 Wrzesiński, D. and Paluszkiwicz, R.: Spatial differences in the impact of the North Atlantic  
912 Oscillation on the flow of rivers in Europe, 42, 30–39, <https://doi.org/10.2166/nh.2010.077>,  
913 2011.
- 914 Wu, Y., Zhang, G., Shen, H., and Xu, Y. J.: Nonlinear Response of Streamflow to Climate  
915 Change in High-Latitude Regions: A Case Study in Headwaters of Nenjiang River Basin in  
916 China's Far Northeast, *Water*, 10, 294, <https://doi.org/10.3390/w10030294>, 2018.
- 917 Yuan, X., Zhang, M., Wang, L., and Zhou, T.: Understanding and seasonal forecasting of  
918 hydrological drought in the Anthropocene, *Hydrol. Earth Syst. Sci.*, 21, 5477–5492,  
919 <https://doi.org/10.5194/hess-21-5477-2017>, 2017.
- 920 Zhang, W., Mei, X., Geng, X., Turner, A. G., and Jin, F.-F.: A Nonstationary ENSO–NAO  
921 Relationship Due to AMO Modulation, *J. Clim.*, 32, 33–43, <https://doi.org/10.1175/JCLI-D-18-0365.1>, 2019.



923 Zhang, X., Jin, L., Chen, C., Guan, D., and Li, M.: Interannual and interdecadal variations in  
924 the North Atlantic Oscillation spatial shift, *Chin. Sci. Bull.*, 56, 2621–2627,  
925 <https://doi.org/10.1007/s11434-011-4607-8>, 2011.

926